

Chapter 46

Floods and Droughts in Asia, Europe, and America

Hiroshi G. Takahashi¹, Masashi Kiguchi², Shiori Sugimoto³

¹Tokyo Metropolitan University

²Institute for Future Initiatives, The University of Tokyo

³Japan Agency for Marine-Earth Science and Technology

April 2022

Chapter 46

Floods and Droughts in Asia, Europe, and America

Contents

46 Floods and Droughts in Asia, Europe, and America	1
46.1 Introduction of Flood and Drought	1
46.2 Water and energy cycles for the understanding of flood and drought . . .	3
46.3 Characteristics of flood	4
46.3.1 Regional floods	5
46.3.2 Flash floods	5
46.3.3 Ice-jam floods	6
46.3.4 Storm-surge floods	6
46.3.5 Mudflow flood	6
46.3.6 Historical record of flood	6
46.4 Characteristics of drought	7
46.4.1 Meteorological drought	8
46.4.2 Hydrological drought	8
46.4.3 Agricultural drought	8
46.4.4 A feedback mechanism between meteorological, hydrological, and agricultural droughts	8
46.4.5 Basic knowledge of drought indices of droughts	9
46.4.6 Drought indices	10
46.5 Precipitation datasets	11
46.5.1 Long-term land precipitation data from rain-gauge precipitation and their merged archives	12
46.5.2 High-resolution land precipitation data from precipitation-radar .	12
46.5.3 Long-term global or quasi-global precipitation from rain-gauge and satellites	12
46.5.4 High-resolution precipitation derived from numerical models . . .	12

46.6	Various scales of flood and drought	13
46.6.1	Various spatial scales of flood	14
46.6.2	Regional characteristics of floods and the relationship between the orographic factors	14
46.6.3	Drought and heatwaves and related to air pollutions	14
46.7	Past floods and droughts and associated meteorological phenomena . . .	15
46.7.1	Global features	15
46.7.2	Floods, Drought and Heatwaves in East Asia	17
46.7.3	Floods in Southeast Asia	20
46.7.4	Drought in Europe	21
46.7.5	Droughts in America	23
46.8	Summary	24

Abstract

This chapter introduces flood and drought through the understanding of the water cycle. In addition to the water cycle, we consider the energy cycle. The floods and droughts have strong regional and seasonal characteristics. The causes of the unbalanced water conditions can occur under the various meteorological phenomena, which have strong regional and seasonal varieties. For an understanding of the cause of floods and drought, we first consider the geographical characteristics of the floods and droughts. At the same time, we focus on the spatial and temporal time-scale of the flood or drought. Moreover, because floods and drought can be considered as excess and shortage of water, respectively, they are opposite. However, their spatial and temporal scales are asymmetric.

Keywords: Climatic zone, seasonal and regional differences, precipitation characteristics, temporal and spatial scales

46.1. Introduction of Flood and Drought

This section explains the flood and drought in Asia, Europa, and America in terms of meteorological and climatological scientific viewpoints. To understand more practical countermeasures against floods, it is also better to see a hydrological handbook.

Generally, floods and droughts have severe impacts on society all over the world. To understand the floods and droughts, we should understand the concepts of "hydrological balance", which can be simply explained by the difference between the input and output of water on a considering area (Fig. 1), such as a watershed and a part of a watershed. When the input of water into the considering area is larger than the output of water, the mass of water must be increased and, in turn, can induce a flood. On the other hand, if the input is smaller than the output, a drought condition may occur. To understand the "hydrological balance" in the considering area, we should understand the hydrological cycle. The hydrological cycle has many processes, such as Ocean precipitation, Ocean evaporation, water vapor transport, land precipitation, evaporation, transpiration, surface flow, percolation, groundwater flow (Fig. 2). In addition, we have to think of the balance of energy as well as the balance of water (Fig. 2).

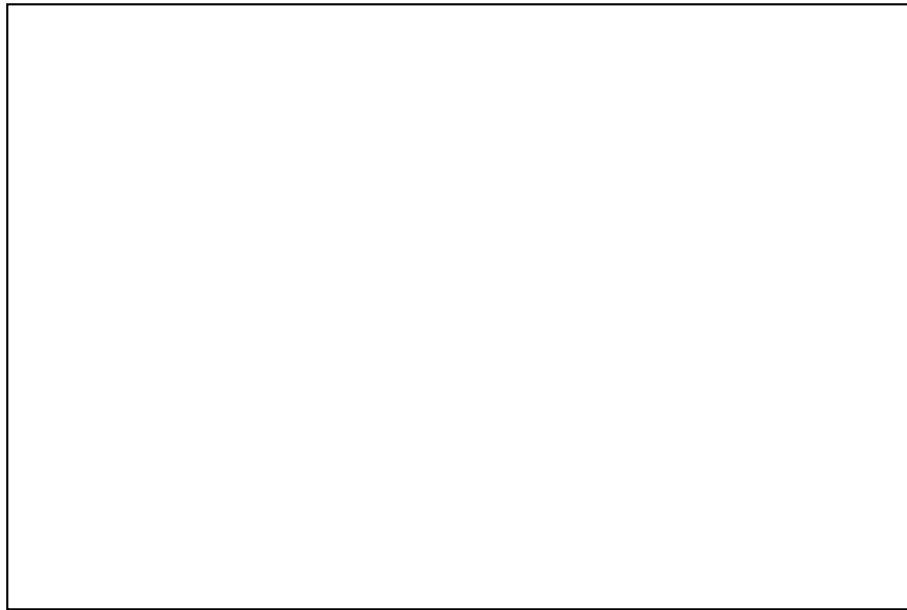


Figure 46.1: *Figure omitted due to copyright. See: Trenberth et al. 2007.* Schematic of the local atmospheric water balance. The large arrows indicate atmospheric moisture divergence, which is mostly compensated for by evapotranspiration E and precipitation P , as changes in atmospheric moisture storage are small. At the surface $E - P$ is balanced by surface and subsurface runoff, and changes in soil moisture and groundwater. (Citation: Fig. 2 of [1] Trenberth et al. 2007)

The inputs of water are basically direct precipitation flux in the vertical direction from the atmosphere, and surface flow and underground water flow in the nearly horizontal direction. The outputs of water are basically evaporation fluxes from the land or water

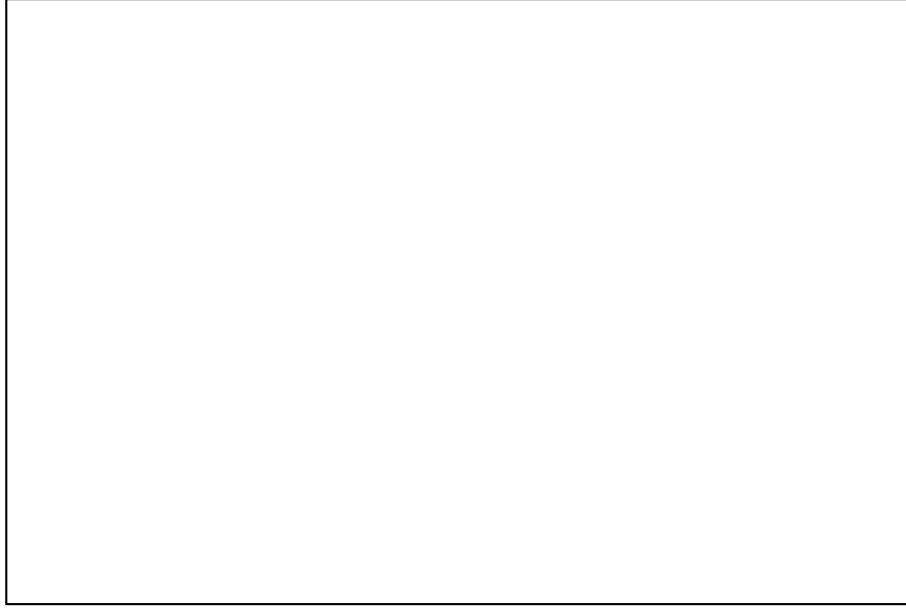


Figure 46.2: *Figure omitted due to copyright. See: Trenberth et al. 2007.* The hydrological cycle. Estimates of the main water reservoirs, given in plain font in 10^3 km^3 , and the flow of moisture through the system, given in slant font ($10^3 \text{ km}^3 \text{ yr}^{-1}$), equivalent to Eg (10^{18} g) yr^{-1} . (Citation: Fig. 1 of [1] Trenberth et al. 2007)

body from the considering area, surface flow, and groundwater flow into the out of the considering area. However, all physical processes, such as precipitation, surface flow, are very complicated to monitor, understand and predict the individual components, and the quantification of the total budget of water is still very difficult.

In addition to this, we should consider the temporal and spatial scales of the physical processes over the world. Such a flash flood generally in a shorter time scale than one day, short-time (time-scales from tens of minutes to hours) and heavy precipitation, and surface flow may be essential drivers. Some other processes, such as evaporation from the surface and underground flow, can be quantitatively negligible because the terms of evaporation and underground flow are much smaller than those of precipitation and surface flow. However, this flash flood may occur at the small spatial scales, which cannot induce a continental scale flood. When we consider a continental scale flood, large-scale atmospheric processes can be a significant driver, such as tropical storms, mid-latitude low-pressure systems, and mid-latitude frontal systems.

On the other hand, drought can be due to a lack of water. Over the tropics, El Niño Southern Oscillation (ENSO) can induce a long-lasting (more than one month) drought. Over the mid-latitude regions, atmospheric blocking high, which generally lasts a few weeks, can induce a continental scale drought. It is noteworthy that the spatial scales of droughts are generally larger than those of the floods. In addition to this, the temporal scale of droughts is longer than that of floods. Moreover, droughts are generally associated with heatwaves.

Here, it should be noted that floods and droughts can be the opposite phenomenon because the excess water in the considering area can induce a flood, and the water shortage in the considering area may induce a drought. However, they are clearly asymmetric on temporal and spatial scales. Thus, physical phenomena can be the opposite; however, they should not be so simple.

The concept of geography is quite essential to understanding floods and drought. The atmospheric and meteorological characteristics have a strong dependence on the regions. Air temperature, humidity, and winds are quite different among the climatic regions, which is associated with floods and droughts. For example, in the tropics, tropical storms can be a significant factor. In the mid-latitude regions, mid-latitude low-pressure systems and mid-latitude frontal systems should be considered, although mesoscale precipitation systems embedded in the large-scale atmospheric systems may be critical in some cases.

Also, land surface conditions, such as soil and vegetation conditions, can be associated with floods and droughts, although they are also related to the climate, as seen in the Köppen climate zone. The coefficient of water permeability of the land surface is associated with the output of water from the considering area. Vegetations enhance transpiration, which also affects the water budget of the considering area. In addition, human-induced changes in land surface conditions, such as urbanization and cultivation, strongly influence the water budget of the considering area. However, because the human-induced changes of land surface conditions are a wide range of variations, we discuss the impacts in the minimum necessary.

Moreover, small and large-scale topographies should be considered. This is because the hydrosphere response is quite different under the different topographic conditions, even if the same heavy precipitation event occurs. Thus, this chapter also provides the characteristics of flood and drought, focusing on the different responses of flood and drought due to the regional and seasonal differences. We should understand future regional predictions for deepening scientific knowledge and decision-makers.

46.2. Water and energy cycles for the understanding of flood and drought

Flood and drought can occur due to an imbalance of water and energy over a target region. The spatial and temporal scales of the imbalances are dependent on the flood and drought events. The imbalance can occur under the anomalous atmospheric circulations, such as short-duration heavy precipitation, abundant seasonal precipitation, a development of the drier weather than usual due to a blocking high, and so on. The anomalous atmospheric circulations are associated with the regional characteristics of climatology.

The imbalance of surface water directly explains the floods and droughts. In addition to the imbalance of surface water conditions, the imbalance of surface energy is closely related to the imbalance of surface water conditions. This is because the term of the latent heat flux in the surface water budget is tied with the redistribution of the surface available energy, which is derived from the shortwave radiation (solar radiation) and longwave radiation (atmospheric radiation).

Specifically, under drier surface water conditions, more energy is used for raising the surface air temperature. In this situation, less energy is used for the vaporization of surface water, which in turn relatively decreases atmospheric water vapor. In the actual cases, the redistribution of the surface energy is related to the surface air temperature in the target conditions. There is a temperature dependency of the redistribution of the surface energy. More specifically, in higher temperature conditions, more energy is used for vaporization. This can also be explained by using the Bowen ratio in some cases. Bowen ratio (Bo) is defined as the non-dimensional ratio of sensible heat divided by latent heat ($Bo = H / L_e E$). Here, H is sensible heat, which is used for the rising temperature, L_e is latent heat required for water evaporation, and E is vaporized water.

A larger (smaller) Bo value indicates that H is relatively larger (smaller) than $L_e E$, which implies that the land surface condition is dry (wet). Thus, the Bowen ratio is a useful value to understand the surface water conditions.

Feedback mechanisms are also very important to understand floods and droughts. The specifics of the feedback process will be explained in the following parts. As a result of the redistribution of the surface water and energy, atmospheric conditions and circulations are modified on the regional scales, particularly in the downstream regions. The changed atmospheric conditions can modify the water and energy budget in the target regions. This can be more significant in the case of droughts. For example, when some trigger causes a rising surface air temperature, additional rising surface air temperature can occur. Warmer surface air temperature condition accelerates evaporation, and surface water condition becomes drier than cooler atmospheric conditions. The drier surface can use the surface energy for the rising surface air temperature. This series of processes can be repeated as positive feedback, which in turn induces drought conditions. To quit from this loop, another external forcing, such as a low-pressure system, is necessary. However, a high-pressure system, such as a mid-latitude blocking high, may block the intrusion of the water supply, which enhances the warm-dry feedback loop.

For understanding the flood and drought, imbalances of water and energy should be considered simultaneously. In addition, it should be considered how the atmospheric processes can accelerate or deescalate the imbalance conditions at multiple spatial and temporal scales.

46.3. Characteristics of flood

A flood is one of the natural disasters and a major problem in a wide area of the world. In 2020, EM-DAT (Emergency Events Database) reported 389 natural disasters killing 15,080 people, affecting 98.4 million others, and costing 171.3 million US\$ ([2] EM-DAT, 2021). Compared with the previous two decades (2000-2019), there were 26% more storms than the annual average of 102 events, 23% more floods than the annual average of 163 events, and 18% more floods than the annual average of 5,233 deaths. These impacts of the events were not equality of location where it occurred. The impacts of floods were heavily throughout Africa and Asia. In Africa, floods affected 7 million people and caused 1,273 deaths, the highest figure since 2006. In South and Southeast Asia, monsoon flooding associated with landslides frequently affected some million people. China also has been damaged by significant flooding, and economic loss increases due to recent economic growth.

Flooding is divided into six categories by the United States Geological Survey (USGS) ([3] Burt, 2004). These six categories are as follows.

- ***Regional floods*** – where a river overflows its banks on a large scale, flooding entire regions.
- ***Flash floods*** – when an intense local rainfall causes a stream or river to suddenly flood a small area, usually the local watershed of that river.
- ***Ice-jam floods*** – when melting ice-floes dam a portion of a river, normally in the spring, causing it to flood upstream from the ice blockade.

- ***Storm-surge floods*** – when a sudden rise in the sea level inundates coastal areas, usually during intense typhoons prior to the landfall of the eye. Also happens on a lesser scale from intense storms of a non-tropical nature.
- ***Dam failure floods*** – often the result of faulty engineering.
- ***Mudflow flood*** – when the ash from a volcanic eruption washes into rivers and creates mudflow-like conditions.

Of the above, dam failure flood is out of scope in this chapter. Most dangerous floods are those caused by storm surges during Typhoons (e.g., Typhoon Haiyan in November 2013) and flash floods caused by intense local rainfalls (e.g., Uttarakhand in North India in June 2013). The typhoon forecast has recently improved more, while the forecast of the pass way of typhoons is still difficult. Storm surge by typhoons is strongly affected by pass way because the relationship between the wind direction, and the coastal line, and the 3-dimensional shape of the gulf affect the scale of the storm surge strongly. Moreover, the simulation for storm surges has large uncertainty. On the other hand, no one knows of any possible floods as the cause of flash floods since it is not always necessary to have intense rainfall in the area where the flood occurs. Moreover, the lead time for evacuation from the flash flood is not enough due to the rapid impact on that.

46.3.1. Regional floods

Regional floods are more destructive than, but usually not as deadly as, flash floods. Rainfall has fallen continuously in the period from a few days to a few weeks, or seasonal rainfall amounts are very abundant in a wide region. As a result of the abundant precipitation, flooding occurs slowly rather than flash floods. Continuous rainfalls are provided by the strengthened trough or front and by the active monsoon rather than the normal on a large scale. Regional floods cause widespread property damage and can result in large death tolls. Recently, the typical regional flood occurred in the Yangtze River basin, located in southern China in 2020, and resulted in around 400 deaths and property damage of 21.8 billion US\$ ([2] EM-DAT, 2021). Heavy rainfalls caused by the Meiyu (regional rainy season) led to floods severely affecting large areas of southern China.

46.3.2. Flash floods

Flash floods are rapid flooding of lower places below the surrounding area (i.e., valleys, including rivers). It might be caused by heavy rainfall associated with storms (i.e., tropical cyclones, thunderstorms, melting water from snow or ice). Flash floods may also occur by collapsing natural debris or ice dams. The intensity of rainfall, the location and distribution of the rainfall, the land use and topography, vegetation types and growth/density, soil type, and soil water-content all determine just how quickly the flash floods may occur and influence where it may occur ([4] National Weather Service, 2021). For instance, flash floods occurred in Jakarta (capital of Indonesia) and its metropolitan area on January 1, 2020, due to the heavy overnight rainfall, causing the overflow of the rivers. The death toll is over 60.

46.3.3. Ice-jam floods

An ice jam occurs when chunks of ice clump together to block the flow of a river. It can cause flooding near the river. These are caused by snow/ice melting water in the spring season, and warm temperature and rainfall in this season cause snow and ice to melt rapidly. This additional water makes the river discharge increase, and this stream carries an amount of ice chunks downstream. Some ice chunks may be stuck in a narrow width of the river, then these ice chunks form an ice jam, which blocks the river flow. This flooding often occurs in Siberia, northern Europe, and the northeastern American continent. Ice-jam flood in Ob River in Siberia commonly occurs and affects the infrastructures related to human activities ([5] Papa et al., 2007).

46.3.4. Storm-surge floods

Storm surge is a rise of water generated by a storm over and above the predicted astronomical tides. It should not be confused with storm tide, which is defined as the water level rise due to the combination of storm surge and the astronomical tide ([6] NOAA, 2021). It is known that storm surge is produced by water being pushed toward the shore by the force of the winds moving cyclonically around the storm. So, the storm's air pressure and traveling direction are important elements for storm surge. Along the coast, storm surge is often a huge impact on human life and property by tropical cyclones (typhoons, cyclones, and hurricanes developed in the northwestern Pacific Ocean, Indian Ocean and the southern Pacific Ocean, and the northeastern Pacific Ocean and the Atlantic Ocean, respectively). According to EM-DAT, the "Bhola" cyclone in 1970 had attacked East Pakistan (present-day Bangladesh) and West Bengal state in India and caused the storm surge flooding. At least 500,000 people were killed by mainly storm surge floods around the lower area, including islands of the Ganges Delta.

46.3.5. Mudflow flood

Mudflow is a geological phenomenon in which water includes masses of soil and rock, rush down the slopes, and a very rapid to the extremely rapid surging flow of saturated plastic soil in a steep channel, involving significantly greater water content relative to the source material ([7] Hungr et al., 2014). Compared with rock avalanche and debris flows, the size constituent particles are small. Triggers of mudflow might be heavy rainfall, snowmelt, volcanic eruption, earthquake, and so on. The largest historic mudflow occurred by the eruption of Mount St. Helens, a volcano in the state of Washington, the USA, in 1980. The volume of material displaced was 2.8 km³.

46.3.6. Historical record of flood

Here, the historic recorded floods are introduced based on EM-DAT and [8] Gunn (2008). Record of extreme meteorological phenomena is important for recognition of what would occur in the future. EM-DAT set the criteria of disaster; 1) 10 or more people dead, 2) 100 or more people affected, 3) The declaration of a state of emergency, and 4) A call for international assistance. Following records follow these criteria.

Worst historic flood occurred by the abundant rainfall during the rainy season (July-August) in Yangtze and Huai river basins in 1931. Death toll is estimated of 3.7 to 4.0 million ([9] Coutney, 2018).

Second worst occurred by the breaking dike of the Yellow river in September 1887. Death toll is at least 0.9 million, highest estimated death toll is 2 million (e.g., [8] Gunn, 2008). Flood water spread quickly throughout the North China Plain, covering an estimated 130,000km² ([8] Gunn, 2008).

Third worst one occurred by the storm-surge due to the 1970 Bhola cyclone that attack East Pakistan (present-day Bangladesh) and West Bengal state in India on November 11, 1970. Death toll is at least 0.5 million due to mainly storm-surge for the lower Ganges delta including small island. The surge height was about 10 meters ([10] Kabir et al., 2006).

Forth worst one occurred by the storm-surge due to the 1839 tropical cyclone that attack southeast India on November 25, 1839. Coringa located in Andhra Pradesh State of India suffered huge damage by strong wind and a large storm-surge (about 12 meters), and death toll is around 0.3 million. Coringa has destroyed completely, then people moved to far inland.

Fifth worst one occurred by the rainfall during rainy season along the Yangtze River basin in July 1935. Death toll is around 145,000 (EM-DAT). China has not recovered from 1931 Yangtze food. As a result of this, the remaining flood relief infrastructure which included damage reservoirs and flood water channels were soon overwhelmed.

Top 5 worst disaster of floods are introduced so far. Here it is shortly introduced that we exclude the floods from the historical floods list, even though the death toll is rather than 0.2 million. Reason of excluding is those floods occurred by human activities such as war and dam failure.

First one is the 1938 Yellow River flood, named as "Huayuankou embankment breach incident", created by the Nationalist Government in central Chida during the early stage of the second Sino-Japanese War to halt the rapid advance of Japanese forces. Death toll (not including military loss) is around 0.4 – 0.9 million ([11] Muscolino, 2014). Until the dike was rebuilt in 1947, the mainstream of the Yellow River flow down to Huai River, and the farmers on that area suffered frequent flood and famine.

Second one is the 1975 Banqiao Dam failure in August under the influence of Typhoon Nina. Death toll is 26,000 – 240,000 with huge inundation area (about 12,000km²) ([12] Xu et al., 2008). Two major dams, including Banqiao Dam, two medium dams, and small 58 dams failed from overtopping in the storm.

46.4. Characteristics of drought

Generally, three types of droughts have been defined. The following subsections provide general categories of droughts. However, the three types of droughts are not always independent. The classification is based on the areas, sections, or society of the influence. In addition, even when there are similar meteorological and climatological forcing associated with the droughts, the response of climates varies by region.

The conditions for a drought of occurrence vary from region to region. For example, the forcing of a monthly precipitation anomaly from the normal climate conditions -50 mm is significant over semi-arid regions. In contrast, it has a small impact on wet tropical regions. In meteorology and climatology, we frequently use the anomaly from the normal year or ratio to the normal year because the spatial distribution of a meteorological variable, particularly precipitation, shows strong non-uniformity. Note that the climatological values are generally calculated to be averaged meteorological variables, such as precipitation, surface air temperature, for a 30-year period. As a side note, in a

world undergoing climate change, the determination of climatological values can also be a major issue.

46.4.1. Meteorological drought

A prolonged less precipitation condition than the normal condition over a target region is generally understood as meteorological drought or simply a drought. The meteorological drought condition is simply understood as an imbalanced water condition at the surface. Thus, an occurrence of a meteorological drought can be found from precipitation observation if we have precipitation observations over the target region. However, understanding past meteorological droughts, for example, is often hampered by the limited availability of precipitation observations.

In general, we can explain that a time scale of an occurrence of the meteorological drought is longer than a few weeks. However, it should be noteworthy that it highly depends on the climate conditions of the target region. At least, most time and spatial scales of drought conditions are longer and broader than their flood conditions when we consider the same target region. Many cases of drought are accompanied by heatwaves, and the two may not always be distinguishable.

46.4.2. Hydrological drought

Due to a meteorological drought or a long-term continuity of meteorological drought conditions, hydrological conditions become drier than a normal condition of a target region, such as surface flow, groundwater levels, and soil moisture content. Because the time constant of the hydrosphere is generally longer than that of the atmosphere, hydrological droughts take longer to occur than meteorological droughts.

46.4.3. Agricultural drought

Meteorological drought and/or hydrological drought results in adverse effects on the crop and vegetation. Under the higher surface air temperature and/or drier soil moisture conditions, the plants are not able to use the water they need, and they are not able to do enough transpiration. The meteorological drought and hydrological drought conditions are associated with the prolonged fewer precipitation conditions. The less active vegetation conditions may also affect the atmosphere in the near future if precipitation occurs later due to the decrease of the function of the transpiration of the damaged plants.

46.4.4. A feedback mechanism between meteorological, hydrological, and agricultural droughts

Drought events are mostly related to meteorological droughts, hydrological droughts, agricultural droughts, and heatwaves. In addition, there is a feedback mechanism between the meteorological, hydrological, and agricultural droughts. When the soil moisture content decreases than normal conditions, the drier surface condition can, in turn, increase the surface air temperature through the changes in the surface heat and moisture fluxes. As a result, the drier surface conditions with the higher surface air temperature, which are sometimes heatwave conditions, can result in further drought conditions with much higher surface air temperature. This feedback is crucial in drought. To escape from the

feedback process associated with droughts, external forces such as precipitation events are necessary.

46.4.5. Basic knowledge of drought indices of droughts

This subsection explains the basic knowledge behind the drought indices. Useful indices are introduced in the following subsections based on the previous review ([13] Seneviratne et al., 2012). For a scientific understanding of the droughts, the following fundamental meteorological values can deeply understand the detailed physical processes and temporal evolution of the climate conditions related to the droughts.

To understand the drought conditions over the world, many indices can be used ([13] Seneviratne et al., 2012). Some indicators are simply understandable and easy to monitor the meteorological conditions if real-time or quasi-real-time monitoring can be provided over the world. Currently, satellite observations of the surface of the Earth can provide global information of surface conditions.

Drought can be characterized as the surface air temperature conditions and surface water conditions. In general, a drought condition is one in which the ground surface temperature is high, or the ground surface is dry.

During a drought period, surface air temperature is generally higher than normal conditions. An anomaly from the climatological surface air temperature, for example, January surface air temperature, is much higher, which indicates a possibility of drought. However, it is dependent on the climatological features. Thus, surface air temperature can be an indicator of drought conditions. However, it is not easy to determine the surface air temperature from satellite observation. To estimate the spatial distribution of the surface air temperature from the satellite observations, it is necessary to be fitted with some kind of numerical model (physical or statistical).

As an indicator of the surface water condition, the surface temperature, which is the skin temperature of the surface of the Earth, is available. It is important to note that "*surface temperature*" and "*surface air temperature*" are two completely different variables, although the surface temperature looks similar to the surface air temperature. Surface temperature is more largely affected by surface water conditions than the surface air temperature. When the water in a near-surface soil layer is small, the surface temperature increases rapidly because of the surface energy and water balance ([14] Seneviratne, S. I., et al. 2010). When the energy is supplied to the surface as downward solar radiation (In meteorology and climatology, and related sciences, visible radiation is called short-wave radiation, here, this is a contrast with infrared radiation, i.e., longwave radiation. This is because the wavelength of visible radiation is shorter than the wavelength of infrared radiation.), the energy should be redistributed into the energy for the increase in the surface temperature and surface water evaporation. When surface water is smaller, more available energy at the surface is used to increase in surface temperature, which in turn increases the surface air temperature through the atmospheric turbulence in the atmospheric boundary layer. Thus, the surface temperature can be an indicator of the surface water condition. However, the response of surface temperature to the surface water condition is not simple. Under the condition of the shortage of surface water, the surface temperature rapidly increases. Under the abundant surface water conditions, the increase in surface temperature is suppressed due to evaporative cooling.

As another surface water condition, surface wetness has been observed from the satellite observations. For example, using a passive microwave imager on satellites (e.g.,

Advanced Microwave Scanning Radiometer 2 (AMSR2)/Global Change Observation Mission - Water Satellite 1(GCOM-W1)) surface water conditions can be obtained around the world. This type of observation is relatively new, which has been available since the end of the 20th century. The surface wetness is an indicator of the drought condition. As well as the surface temperature, the climatological condition in surface wetness is geographically different. Thus, we should also use anomalies of surface wetness for monitoring drought conditions.

It is well known that precipitation is a good indicator of drought conditions. Even today, rain gauges play an essential role, but there are many areas where rain gauges are not available, and there are many aspects of forecasting and monitoring that cannot be covered by rain gauges alone. However, direct observation of the spatial distribution of the precipitation is very limited. For example, the core satellites of the Tropical Rainfall Measuring Mission (TRMM) and the Global Precipitation Measurement (GPM) have radar observations from space. However, high-latitude regions are out of the measurements. To estimate the precipitation distribution, cloud information has been used for many years as an alternative to precipitation, although it is difficult to monitor precipitation quantitatively from cloud information. Currently, several datasets of precipitation are distributed, which will be introduced in the following section. Also, other drought-related indices are introduced below.

46.4.6. Drought indices

While the surface temperature, soil wetness, and precipitation presented in the previous section are themselves useful indicators of drought, a variety of other indicators are also used. Other drought indices have been summarized in the review [13] (Seneviratne et al., (2012) of *"Box 3-3 The Definition of Drought"*. Basically, they introduced three types of drought indices, indices calculated from only precipitation dataset, ones calculated from precipitation and potential evaporation dataset, and ones calculated from more complicated numerical models. For practical use purposes, some simple drought indices are introduced here.

The first index is the consecutive dry days (CDD). This CDD index is quite simple to count the consecutive days that have no precipitation. This CDD index can be calculated from the daily precipitation of observation and a climate simulation. CDD is quite simple but reasonably practical for the analysis of the drought. In the context of climate change, the CDD may change in the future. Because the long-lasting dry days can induce a drought, the longer CDD increases the risk and impact of the drought. Generally, the drought tends to be severe due to the long-lasting dry conditions because soil conditions can close to the shortage of soil moisture for evaporation. However, it may not be useful for dry regions because dry days continue for several ten days, even in normal climate conditions.

Also, soil moisture anomalies (SMA) are useful. SMA is easy to understand the condition of soil moisture. If the SMA can be monitored, the shortage of soil moisture, which induces the drought condition, can be found. The SMA is also quite useful for analyzing the climate model simulations because most climate models coupled with land surface models and the soil moisture values are outputted. What time-scale SMA to analyze depends on the climate of the region, but SMA on time scales longer than a week is often examined. However, there is a problem with the limited period of SMA data for analysis of past soil moisture observation data. Compared with the precipitation or

temperature data, the soil moisture data has been limited. In addition, the observation data before the satellite observation era are spatially limited. Generally, soil moisture conditions are quite significant heterogeneity in space and depth. Thus, the SMA is useful but is not available depending on the research purpose.

As a drought index calculated from precipitation and potential evaporation datasets, the Palmer Drought Severity Index (PDSI) ([15] Palmer, 1965), which measures the difference of moisture balance from normal climate conditions using a simple water balance model (e.g., [16] Dai, 2011), is well known and commonly used. However, estimating the potential evaporation is not so simple because it is difficult to observe. In addition, the target time-scale of PDSI can be more than one year. Thus, PDSI is used for long-term droughts, such as a multiyear drought.

In addition, many researchers have proposed and studied many drought indices, focusing on regional drought events. However, the usefulness of the drought indices should be considered over the target regions. As the CDD may not be useful over the dry climate regions, individual indices have advantages and disadvantages, which should be related to the regional climate conditions.

46.5. Precipitation datasets

This subsection introduces the current precipitation datasets in terms of the characteristics of temporal and spatial coverages. To monitor and understand floods and droughts, these precipitation datasets are essential. Without the observational datasets, we cannot monitor, understand and discuss the current and past statuses of the flood and drought. Thus, the precipitation datasets are the most significant resources for flood-and-drought predictions and research.

In addition, precipitation observations have evolved in recent decades from direct observation by the offline rain-gauge networks to the near-online remote sensing (radar, microwave imager, infrared imager, and so on) precipitation or their mixtures. The characteristics of individual precipitation datasets are different, including the uncertainty of the dataset.

As shown in below, various kinds of precipitation datasets are available. If the target is flash flooding associated with heavy rainfall events on small spatial scales and short time scales, products based on precipitation radar and recent satellite data are suitable. On the other hand, if the target is a long-term drought or a long-term variability of droughts, it is necessary to use long-term homogeneous precipitation data, although the spatial resolution does not necessarily have to be fine. In general, the shorter time-scale and spatially higher-resolution precipitation datasets are often not suitable for analysis of long-term variation, as it often does not give much consideration to long-term homogeneity of data quality. On the other hand, long-term data often have a coarse resolution in space and time and are not suitable for the analysis of phenomena with short time scales and small spatial scales, such as flash floods and short-duration heavy rainfall. Although a large number of precipitation data exist, appropriate precipitation data should be selected according to the purpose.

46.5.1. Long-term land precipitation data from rain-gauge precipitation and their merged archives

The classical and long-term precipitation datasets are based on the direct observations by a rain-gauge itself, rain-gauge network, or their archives (e.g., Global Precipitation Climatology Centre (GPCC), [17] Schneider et al. 2008). Many researchers and technicians have devoted themselves to unifying or quality-check the observed data. The primary purpose of the quality checks is to obtain possibly homogeneous datasets in time and space. In terms of a time axis, the qualities are quite important to understand climate change in the target region. If the observational point can be changed, the homogeneity cannot be preserved. In terms of a spatial axis, the qualities are quite important to compare the data between the different observations. If the qualities of the precipitation observations are quite similar, we can use the data for the spatial analysis, which is associated with the construction of rainfall networks.

46.5.2. High-resolution land precipitation data from precipitation-radar

Due to the development of the precipitation radar technique, precipitation-radar networks have been constructed all over the world. The precipitation-radar networks are often operated by the national meteorological agency. Compared with the rain-gauge, the number of meteorological stations can be reduced. However, the observation coverage is closely related to the topography. For example, a valley region cannot be observed from the outside of the valley. There may be other technical problems; temporally and spatially high-resolution precipitation data can be obtained from a precipitation-radar network. Currently, the high-resolution precipitation from the radar can be obtained near-real-time, which is used for flood predictions.

46.5.3. Long-term global or quasi-global precipitation from rain-gauge and satellites

Using many satellite observations, many precipitation products have been developed in a few decades (e.g., Global Precipitation Climatology Project (GPCP); [18] Adler et al. 2017). It started with infrared radiometer observations from polar and geostationary orbit satellites. Using the infrared radiometer, we can understand the cloud activity, which is basically related to the precipitation activity. However, the infrared radiometer can only detect cloud-top information from space. To improve algorithms of the precipitation estimation, other sensors were gradually used for the estimation of precipitation. For example, a microwave imager can detect some cloud and water vapor information; many microwave imagers have been used for the algorithms of precipitation estimation. In the development of the algorithms for precipitation estimation, grand validation is very important. To improve the estimation, ground-based observations are used. Currently, the high-resolution precipitation from the satellites can be obtained near-real-time, which is used for flood predictions.

46.5.4. High-resolution precipitation derived from numerical models

When we use all the satellite observations and radar observations, we cannot predict future precipitation even in a few minutes. To predict future precipitation activity, we use many kinds of numerical models. For example, for precipitation forecasts shorter than

one hour, we can use simple advection models, physical numerical weather models, and other statistical models. Currently, a statistical model can be developed by an artificial intelligence (AI) technique.

To predict near future precipitation in a few hours, numerical predictions can be conducted using well-initialized conditions. For the initial values of numerical predictions, real-time or near real-time observations are used. More accurate predictions can be made by using initial values that sufficiently reflect the current atmospheric conditions obtained from real-time observations.

While there are a lot of valuable datasets, there are also data that are used despite their unreliability and should be used with caution. In the last two decades, atmospheric reanalysis products have been developed (e.g., [19] Kalney et al. 1996, [20] Kobayashi et al. 2015) because of the progress of the assimilation technique and studies with the rapid increase of computational resources.

The well-formatted atmospheric analyses are very useful, which are very similar to the gridded precipitation datasets. It covers the entire globe in more space and time than the data in the gridded precipitation datasets and provides data as if it were available even where there are no past observations. Generally, the gridded precipitation dataset is derived from the past observations, which were interpolated but not extrapolated. Generally, we cannot use the extrapolated precipitation data.

However, when we use the atmospheric reanalysis, we should be careful which meteorological variable is reliable or not. Although the reanalysis has precipitation values, the precipitation values are very uncertain because precipitation values have not been assimilated, i.e., it is the output of the simulation. There is another reason why the precipitation values in reanalysis datasets are unreliable. However, because the explanation is beyond the level of this paper, we briefly explain that unreliability is associated with the uncertainty in the physical model. To begin with, generally, the meteorological element of precipitation cannot be considered to be suitable for assimilation. However, the uncertainties can have been gradually reduced with improvement of the assimilation technique, as the improvement of assimilation of the source of the precipitation, namely water vapor. Nevertheless, the precipitation values in the reanalysis dataset cannot be used as observational data.

In brief, the atmospheric reanalysis is a kind of climate model output, which is assimilated with a lot of observations over the globe. If no observations are assimilated, the reproducibility of the atmospheric reanalysis is quite low. Atmospheric structure and flows are not assimilated with the observational data over the not observation area. Nevertheless, because uncertain atmospheric reanalysis datasets are available, the data is often used without understanding the nature of the data, mistakenly believing it to be accurate. Thus, we should be careful to use the datasets.

46.6. Various scales of flood and drought

Time-scales of flood and drought have a very wide spectrum, which ranges from a few dozen minutes, a few hours, a few days, a few months, and possibly a few years. Generally, the time-scales of floods and droughts have strong regional dependencies. Also, because meteorological characteristics can change seasonally, floods and drought also have strong seasonal dependencies. It should be noted that the time-scales of floods and droughts are not symmetric, even if we focus on a specific region. The opposite of flood is not just drought. Thus, it should be better to discuss them separately.

46.6.1. Various spatial scales of flood

This subsection focuses on floods. In addition to the time-scales, spatial scales of floods are quite important. The range of spatial scales is across a sub-kilometer scale, a few kilometers scale, a hundred-kilometer scale, and a continental scale. Thus, the spatial scales of the floods are also various.

Here, the "spatial scale of floods" is closely associated with the "temporal scale of floods". Mostly, when the spatial scale of a flood is small, the time scale of the flood is small and vice versa. This is very similar to the basic meteorological knowledge of scales between time and space. Thus, for understanding the temporal and spatial scales of floods, it is quite natural that it should be simultaneously focused on both temporal and spatial scales and the target meteorological phenomenon. The target meteorological phenomenon may have the same order of magnitude of spatial and temporal scales of the flood.

46.6.2. Regional characteristics of floods and the relationship between the orographic factors

The regional characteristics of floods are basically associated with the meteorological characteristics of the target regions. However, if the same heavy precipitation occurs over similar tropical regions due to a tropical cyclone, the hydrological responses to the same heavy precipitation have a strong regional dependency. As an example, we will introduce the different regional responses to the tropical cyclone precipitation over the Southeast Asian monsoon regions.

Thailand experienced a severe flood in 2011 (Detailed processes are explained in Section 46.7.3). Similar types of floods can occur over Bangladesh and part of northern India because the topographic and soil conditions are similar. On the other hand, the meteorological disasters in Vietnam and the Philippines are well-known as short-time floods, although their rainfall variability is similarly associated with tropical cyclones.

These differences can be explained by the orographic features. When we look at Asian countries, the orographic characteristics are quite different. Some countries have steep orography, other countries have a broad plain, which is quite gentle orography. In some island countries with steep orography, short-term flash floods occur at relatively shorter time-scales, such as the order of hours. Considering the time for the receding of the flooded water, it takes several days. However, over the flat plains of continents, seasonal floods occur as the seasonal march of climate or had occurred. The time-scale of the floods can be a few months commonly. Some areas have a time-scale intermediate between flash floods and seasonal floods.

Therefore, if the same precipitation occurs over the various orographic regions, the precipitation responses are pretty varied, which can explain the regional differences in floods.

46.6.3. Drought and heatwaves and related to air pollutions

Compared with floods, droughts and heatwaves basically have synoptic or large spatial scales. Thus, the spatial scale of a drought and a heatwave is much larger than the floods over the same target regions. When a heatwave occurs over India, most parts of the country experience the heatwave at the same time. The spatial scales of the droughts

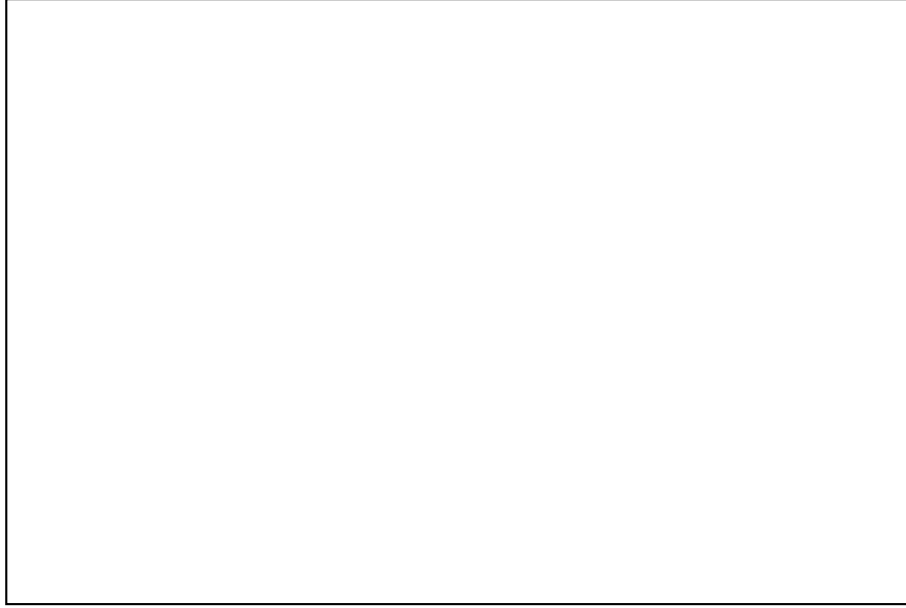


Figure 46.3: *Figure omitted due to copyright. See: Chang et al. 2021.* The atmospheric path of biomass burning-aerosols emitted during the 'Black Summer' from Australia across the Pacific Ocean; aerosol optical thickness (AOT), surface albedo (SA), direct aerosol radiative forcing (ARF) from 1st to 8th of January, 2020. (Citation: Fig. 4 of [21] Chang *et al.* 2021)

and heatwaves are larger than the spatial scale of the country. When a heatwave occurs over western Europe, the heatwave covers multiple countries.

Thus, the spatial scales of the drought and heatwaves are larger than that of the floods. In addition to the spatial scales, the temporal scales range from a few days, a several-day period, to a few weeks, which are longer than that of floods. In some worst cases, the dry period continues across the season, which is associated with not only drought or heatwaves but also large agricultural drought and a large-scale wildfire. In the recent example, 2019–20 Australian bushfire season (Fig. 3), California wildfire season (see also in Section 7.5), and worldwide tropical rain forest fires are huge drought-related disasters, which also provide a large amount of polluted air, namely aerosols and gases. In the 2019–20 Australian bushfire season (Fig. 3), it was clearly found that high aerosol optical thickness (AOT) and negative direct aerosol radiative forcing (ARF) on and over the downstream regions which was induced by the biomass burning over Australia. The biomass burning can be captured by high surface albedo (SA). It is noteworthy that the occurrence of bushfires is strongly associated with the drought in Australia. Thus, drought and heatwaves are also associated with air pollution and climate changes (see also the latter parts of Section 7.1).

46.7. Past floods and droughts and associated meteorological phenomena

46.7.1. Global features

Many studies have reported the long-term changes in floods and droughts. However, the long-term changes in floods are very difficult to evaluate because people have developed

countries against heavy precipitation and floods. Thus, the projections of future floods are also dependent on people's behaviors.

Compared with the floods, the long-term changes in droughts are more related to the large-scale and regional-scale climate changes. The long-term changes in drought have been evaluated, which is closely related to the past climate changes. Thus, it is quite possible that the future changes in droughts are also related to future climate changes. However, it does not intend that the future climate projection is easily possible.

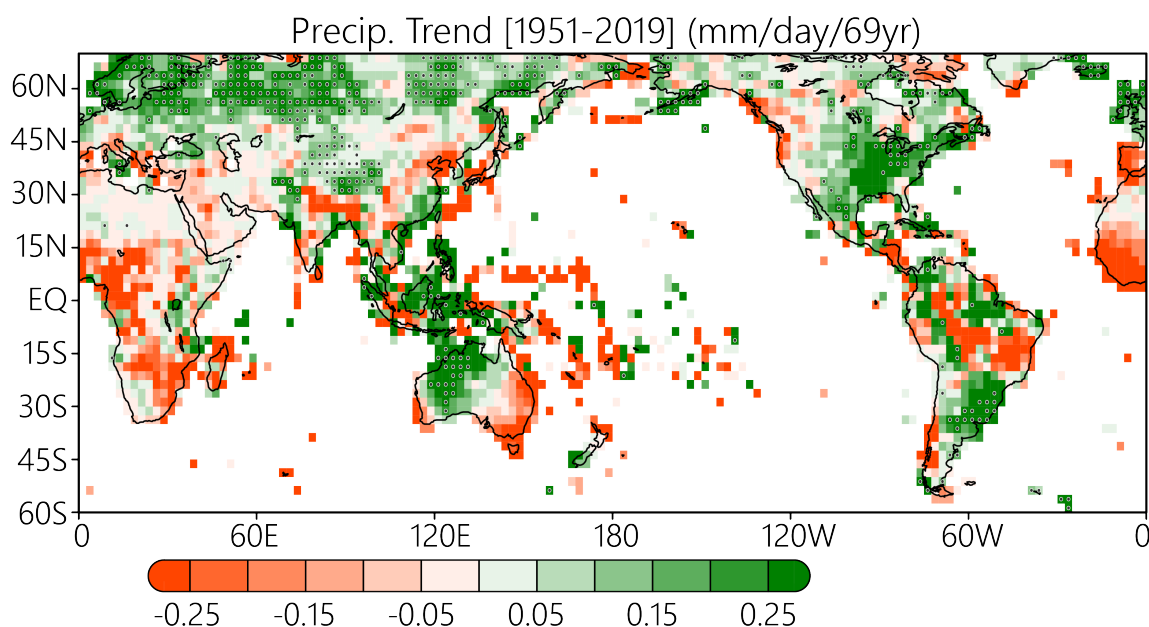


Figure 46.4: Long-term (over 69 years from 1951 to 2019) trends of annual precipitation over land. Used precipitation data was GPCC (see Section 46.5.1 in this chapter). Spatial and temporal resolution is $2.5^\circ \times 2.5^\circ$ and monthly. The unit of the trend is mm/day/69 years. Although values can be seen over the oceanic regions, this data actively uses precipitation observations over islands. The trend values are calculated by Sen's slope estimator, which robustly estimates the trend value with small outlier adverse effects. The dark grey dots denote that the trend values are statistically significant at a 95% significance level, which was determined by the Mann-Kendall trend test with degrees of freedom being 67.

Figure 4 shows the long-term changes in precipitation over the recent approximately 70 years. The long-term changes in precipitation have a regional dependency. For example, decreased precipitation was partly observed in the South, Southeast, East Asian monsoon regions. Over the African Continent, long-term decreases in precipitation were widely observed over the near Equator region, which is well-known as one of the distinct climate changes in the second half of the 20th century. Over western Europe, the Mediterranean Sea region experienced a long-term decrease in precipitation, which is associated

with severe heatwaves. On the other hand, precipitation has broadly increased over the northern region of western Europe. Over the North American continent, the east-west contrast in the long-term changes is quite significant. The drying trends over the western parts of North America can be associated with the recent drought events. A significant decrease in precipitation can be partly seen over the Amazon region, South America. Over the Australian Continent, notable east-west gradients of precipitation trends are observed. The significant drying over the eastern coast of Australia is closely associated with the recent severe Australian bushfire (see Fig. 3 of this chapter).

Parts of these long-term decreases in precipitation were associated with the ENSO variability (e.g., [22] Dai 2013). The extent to which ENSO can explain these trends needs to be further explored.

Figure 5 shows an interannual coefficient of variation of annual precipitation over land. Higher values indicate greater year-to-year variability over the past 70 years, i.e., areas that tend to have severe floods, or droughts, or both. Specifically, high values were calculated over the equatorial Pacific and the Maritime Continent, eastern Africa, the Mediterranean, parts of North and South America, and the Australian Continent. As for the long-term trends in annual precipitation, ENSO variability explains the vigorous interannual variations in precipitation. However, it is quite possible that parts of higher values imply the recent frequent floods and droughts. A similar analysis has been applied for the future climate projection (e.g., [23] Kitoh et al. 1997; [24] Kamizawa & Takahashi 2018), which suggest that wetting projection on the regional scale is not organized in CMIP5 (Coupled Model Intercomparison Project Phase 5) climate models, whereas drying projection can have a tendency to occur widely and systematically. Although there is a random chance in the increasing trend of floods, and it is challenging to accurately predict the areas where floods will frequently occur, the increase in droughts is likely to increase systematically.

It is quite important that air pollution can become seriously related to the drying tendency of future climate changes. The reduction of the effect of wet deposition, an increase of the aerosol emission from natural and artificial biomass burning, and an increase of the aerosol emission from the dried surface can be easy to imagine. Actually, possible feedback between surface drying and aerosol loading was discussed ([25] Yamaji, and Takahashi 2014).

Thus, as mentioned earlier, it is important to note that even with high rainfall (low rainfall), there are areas where flooding (drought) occurs and areas where it does not, as well as timing and time-scales of occurrence. From the perspective of disaster prevention and future projection, regional different disaster preventions against floods and droughts are required because regional problems cannot be solved by global projection alone.

46.7.2. Floods, Drought and Heatwaves in East Asia

Anomalous precipitation is observed over East Asia when the subtropical high develops over the northwestern Pacific and abundant moisture transports along with its anticyclonic circulation. A spatial pattern of global-scale SST over the Pacific and Indian Oceans controls the interannual variability in the subtropical high over the northwestern Pacific (SHNWP), which is well summarized in [26] Xie et al. (2016). For example, an anticyclonic circulation anomaly appears over the surrounding regions of the Philippines in the El Niño winter, which suppresses convection there. This anomaly is maintained during the post-El Niño spring and summer by feedback between SST cooling at its

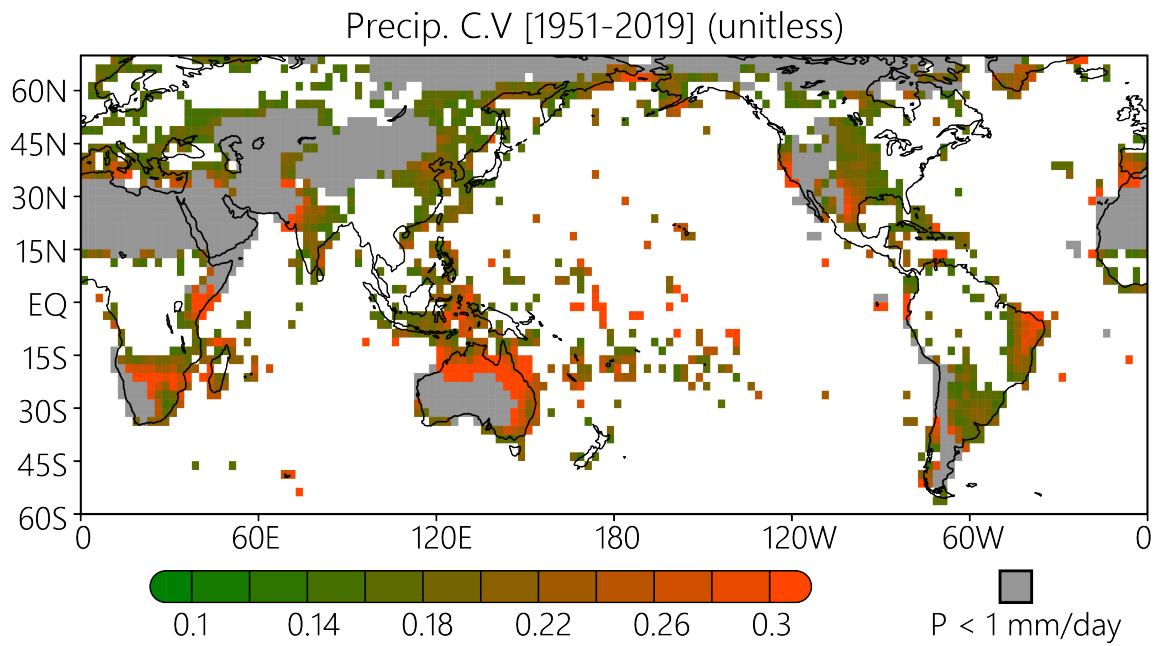


Figure 46.5: Interannual (over 69 years from 1951 to 2019) coefficient of variation of annual precipitation over land. The coefficient of variation is the standard deviation divided by the average value, which indicates normalized standard deviation (dimensionless). A larger value shows that heavy interannual variability, which implies floods and droughts frequently occur. The plotted coefficient of variation is larger than 0.1. The gray shading denotes the annual averaged precipitation is less than 1 mm/day, which can be a dry climate zone. As the reference, the global average (including over the ocean) precipitation is estimated approximately 3 mm/day.

southeastern flank in association with the enhancement of northeast trade wind and a reinforcing of the anticyclonic circulation anomaly by convection suppression over the cool SST. The El Niño also induces the Indian Ocean warming, which acts to anchor the anticyclonic circulation anomaly over the western Pacific until summer. As a result, the SHNWP is intensified in the post-El Niño summer, and an anomalous anticyclonic circulation transports moisture effectively from the tropical Pacific to central-eastern China and southwestern Japan. In addition, a cyclonic circulation anomaly is formed at the north of anticyclonic circulation anomaly, i.e., over northeastern China and central and northern Japan, by a poleward propagation of the Rossby wave called as the Pacific-Japan (PJ) pattern, which activates convection over the Yangtze River basin, Korea, and Japan. Meanwhile, the genesis of tropical cyclone (TC) is suppressed over most of the tropical northwestern Pacific in the post-El Niño summer, and the landfall of TC also reduces eastern China and Korea.

Actually, summer precipitation was extremely high over the Yangtze River valley in 1983 and 1998, of which summers were in the decaying phase of strong El Niño events as well as having the strong warming in the tropical Indian Ocean. The strong El Niño events were also recorded in 2015/2016, and heavy precipitation was observed in June and July, 2016 over the Yangtze River valley; however, precipitation was less in August than the normal due to the enhanced mid-latitude teleconnection, which is referred to as the Silk Road pattern (explained in below). Heavy precipitation lasted during Meiyu/Baiu season in 2020 over China and Japan even though the El Niño was not seen in the previous winter. Although causes of extreme precipitation occurrence in 2020 are investigated by many researchers as of 2021 spring (e.g., [27] Takahashi and Fujinami 2021), the warming in the Indian Ocean associated with the Indian Ocean Dipole mode is considered as a key factor to make such a critical situation ([28] Takaya et al. 2020). In these years, floods and their huge damages are also recorded. For example, the flood that occurred in the 1998 summer led to more than 1500 deaths and economic loss of approximately 255 billion RMB, while the dead and missing people were less than 150 people and economic loss was estimated at approximately 120 billion RMB in association with the 2020 flooding ([29] Wei et al. 2020). Flood disaster is likely to be mitigated by the infrastructure, ecosystem restoration, progress of weather and hydrological forecast technology, and so on.

We also should describe the effect of plateau-scale disturbances generated over the Tibetan Plateau on the heavy precipitation occurrence in East Asia (e.g., [30] Sugimoto 2020). The plateau-scale disturbance is formed during summer by the strong land-surface heating and by a shear line between moist southwesterly winds over the southwestern plateau and northeasterly winds associated with anticyclonic circulation over the northern plateau. A dry-wet gradient in soil moisture is found from northwest to southeast over the plateau, and it increases the occurrence frequency of the plateau-scale disturbances over the western and northwestern plateau. The disturbance generates the mesoscale convective systems (MCSs) over the southern and eastern parts of the plateau, where soil moisture is relatively high. Approximately 25% of the plateau-scale disturbances with the MCS propagate eastward and move out of the Tibetan Plateau, and then, they influence the heavy precipitation occurrence over the upper and middle areas of the Yangtze River basin. Furthermore, the plateau-scale disturbance enhances the Meiyu/Baiu precipitation and causes an abundant moisture inflow toward the Meiyu/Baiu front, which also affects heavy precipitation events over the lower reaches of the Yangtze River and southwestern part of Japan.

On the contrary, extreme hot events with convection suppression occur over East

Asia when a high-pressure anomaly appears there. Climatologically, the western part of SHNWP expands northward and covers East Asia in August, and the South Asian High (SAH) lies in the upper troposphere over Eurasia during summer. The center of SAH is found over the Himalayan regions and oscillates east-west direction with a time-scale of approximately 10–20 days. The Eastern edge of the SAH sometimes extends eastward and reaches over the East Asian countries. The Rossby wave propagation along the Asian jet is a key factor in developing the SAH and the SHNWP. A major Rossby wave train, which excited over the Mediterranean and the Aral Sea, is referred to as the Silk Road pattern ([31] Enomoto et al. 2003). The Silk Road pattern intensifies an equivalent-barotropic ridge structure near Japan. The Rossby wave train induced by atmospheric heating over the Tibetan Plateau also barotropically enhances an anticyclonic circulation over the east of Japan as well as the SHNWP intensification associated with the wave train along with the monsoon westerly in the lower troposphere. For example, extremely hot summers were recorded over Japan in 1994, 2010, and 2013 under the condition of the development of the SAH and the SHNWP. A near-surface temperature averaged over Japan was the highest in 2010 since the record began in 1898, and that record is still unbroken as of spring of 2021. In addition to the continuous hot weather, precipitation was lower than 50% of climatology in Japan except for some regions during the summer of 1994. In this year, water intake from the rivers was regulated in many areas, and water level in Lake Biwa, which is the largest lake in Japan, was the lowest on record. A frequent occurrence of the hot events will also be affected by the global-scale warming, and heat island effect due to the urbanization and foehn at the mountain leeward give a local-scale heterogeneity in the spatial distribution of extreme hot events.

46.7.3. Floods in Southeast Asia

Southeast Asia is consisting of the Eurasian continental portion and islands area. Compared with the mid-latitude zone, there is not so often occurred the catastrophic water-related hazards with abundant death toll, except for storm-surge floods in mainly Philippines.

Based on EM-DAT database since 1900, the deadliest floods occurred by Cyclone Nargis in early May, 2008. Nargis made landfall in low Ayeyarwady delta on May 2 with strong wind, consequently the storm-surge, which height is around 3.5m, claimed at least 138,000 life. Landfall to Myanmar is very rare, and people has not informed because of military administration, are considerable reason of abundant death toll. Second largest case of death toll is Typhoon Haiyan in November, 2013. Haiyan attacked a central part of Philippine with strong wind (more than 60m/s) and storm surge (at least 5-6m), consequently the death toll is 7,354. Philippine, especially, is prone region for typhoon related phenomena such as storm-surge, strong wind, and so on. On the other hand, the death toll is not so much (less than 1,000) in case of riverine flood due to seasonal abundant rainfall rather than the normal. However, the period affected due to flood is longer than that by typhoon or cyclone. Affected period's length directory/indirectly caused in economic loss. Most catastrophic economic damage is 40×10^9 US\$ in case of the Chaophraya River flood in central Thailand in 2011. In case of the 2011 Thailand flood, the largely industrial parks were inundated about a few months. So even though flood speed is slow thus the death toll is small, the economic loss could be huge if high property area is inundated. Flood speed is slow means that the flood water remains a long time. In Southeast Asia, there are three low-lying area in Chaophraya River in

Thailand, Ayeyarwady River in Myanmar, and Mekong River from Cambodia to southern Vietnam. Due to sea level rising by climate change, these areas become more flood-prone region. Recently the urban flood due to the heavy rainfall in short time is focus from the viewpoint of economic issues. Although death toll is about 30 in case of urban flood in Jakarta and Manila, the capital of Indonesia and Philippine, the economic loss list is second and third economic loss in flood case excluding storm-surge. Due to recent economic growth, the abundant properties are accumulated in urban area. When we consider the counter measures of flood in urban, this accumulation of property become one of the important issues.

From here, the meteorological conditions of the Thailand severe floods in 2011 are explained. The meteorological situation of a flash flood due to a tropical cyclone in tropical regions can be easily understood. Here, the meteorological condition of the seasonal flood over Southeast Asia is explained. In 2011, Thailand experienced a severe flood in the Chao Phraya River Basin. This severe flood was due to the active tropical disturbance activity ([32] Takahashi et al., 2015). The time scale of this flood is seasonal, and the excessively accumulated rainfall during the monsoon season induced the flood. To investigate the atmospheric circulations associated with high rainfall, spatial patterns of rainfall variation were identified. The figure shows the regression coefficients plotted against the rainfall variability in the region centered on Thailand, focusing on the severe flooding that occurred in Thailand in 2011 (Fig. 6).

The positive signals were found from northern India, Bangladesh, Myanmar, Thailand, and further to the Philippines, and there is a tendency to have more precipitation in similar years. Because the zonal tilting band corresponded to the significant tropical cyclone path, this result suggests the importance of tropical disturbance activity for the excessive rainfall over Thailand and the flood.

46.7.4. Drought in Europe

Over Europe, severe heatwaves or droughts have been significant problems as an impact of climate change. In 2003 and 2010, the severe heatwaves were the major meteorological and climatological disasters, which may be associated with the current climate changes. As the mean state in the future, severe heatwaves and drought have been projected over and around the Mediterranean Sea. Most "*Fifth Assessment Report of the United Nations Intergovernmental Panel on Climate Change (IPCC-AR5)*" climate models have projected the northward expansion of the Hadley circulation over Europe in the northern summer, which would induce the frequent occurrence of heatwaves or more severe droughts. In addition to the climate changes in the mean state, the interannual variability is associated with respective heatwave and drought events. If the amplitude of the interannual variability is the same as the current climate, the drying trend over Europe enhances respective heatwaves and droughts.

Each heatwave and drought event is associated with the development of a blocking high over Europe. Usually, the blocking high over Europe lasts for one to two weeks, which induces dry and hot conditions, particularly over the inland regions of Europe. However, the location of the blocking and atmospheric circulation varies by heatwave and drought cases. Nevertheless, the spatial scale of the heatwaves and droughts are synoptic rather than regional.

For understanding the heatwaves over Europe, it is essential to consider the land-atmospheric interactions or feedback during a heatwave event. When a blocking high

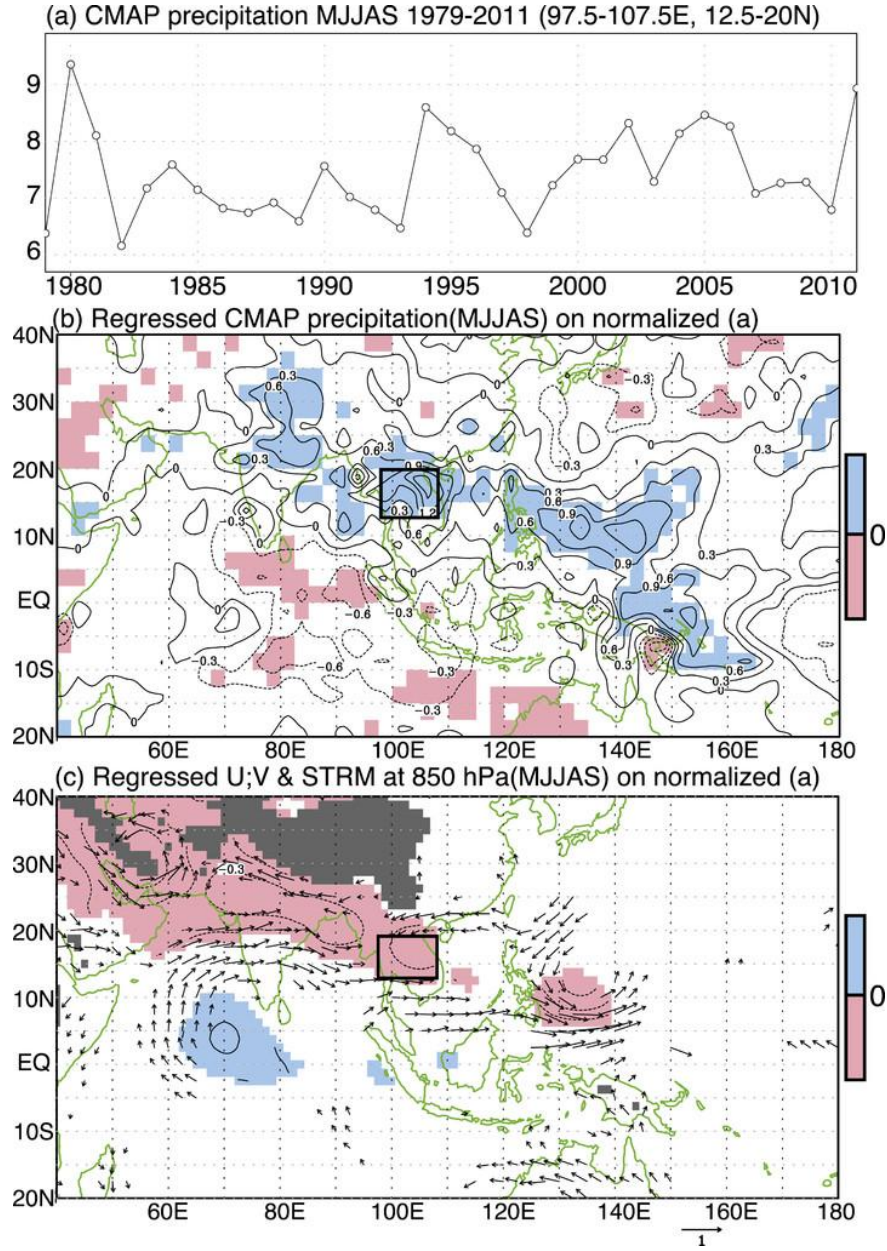


Figure 46.6: (a) Precipitation time series generated from the CMAP dataset for the rainy season (May–September) over the reference region of Indochina (12.5°–20°N, 97.5°–107.5°E) from 1979–2011. The reference region is used for the regression analysis in (b), (c) and is indicated by a solid rectangle in these panels. (b) Regression of CMAP data during the rainy season against the normalized data (mm day⁻¹) shown in (a) from 1979 to 2011. (c) As in (b), but for the 850-hPa zonal and meridional winds and streamfunction (colors) during the rainy season. Areas with colors in (b) and plotted vectors (wind; m s⁻¹) and contours and colors (streamfunction; 10⁶ m² s⁻¹) in (c) are statistically significant at the 90% level, as determined by correlation coefficients based on 31 degrees of freedom (df). (Citation: Fig. 5 of [32] Takahashi *et al.* 2015, copyright 2015 American Meteorological Society)

forms over Europe, surface air temperature increases at first. When the surface air temperature is high, more soil water is consumed to evapotranspiration (summation of soil and water body evaporation and vegetation transpiration). When the soil has some available water, the increase in surface air temperature would be suppressed. However, a long-lasting blocking high can consume much soil moisture. After the shortage of available soil moisture, most of the absorbed solar energy at the surface is redistributed to the sensible heating at the surface, which, in turn, drastically increases the surface air temperature. Moreover, under the condition of the high surface air temperature, the surface is provided with more energy due to an increase in the downward longwave radiation from the atmosphere at the surface in the surface energy budget relationship. Then, the surface must consume more energy to increase the surface air temperature. This land-atmospheric feedback intensifies the heatwaves. Thus, the atmospheric processes and land-atmospheric interactions play a vital role in enhancing heatwaves and droughts.

46.7.5. Droughts in America

Over North America, 2010's had severe droughts, such as California drought or heatwaves. Detailed and more professional review is provided in a recent review paper ([33] Seager and Hoerling 2014). The following description refers to this paper. North America has experienced severe multiyear droughts, such as in 1930's (called Dust Bowl), in 1950's, 1998 to 2004, and 2010's. Although a seasonal drought has been addressed, which can be explained by the Rossby wave propagation forced by the anomalous warm SST over the tropical Pacific Ocean (in the El Niño phase), a multiyear drought had not been able to be explained until 2000's.

The break-through study ([34] Schubert et al. 2004) addressed Dust Bowl drought in 1930's by a large-ensemble experiment (at that time; at the time of writing this handbook, experiments with more than a few dozen ensembles are referred to as large ensemble experiments, but this term may change in the past, present, or future) using an atmospheric general circulation model (AGCM) prescribed the observed SST. A large-ensemble experiment enables us to evaluate the contribution of oceanic impact (SST anomaly) and internal atmospheric and land conditions variability, for example, which can explain that a phenomenon is associated with the land-atmospheric feedback (see Section 4.4 in this chapter). For the multiyear drought, both persistent cold tropical Pacific and warm tropical North Atlantic SST anomalies are the drivers.

As explained in Section 4.4 in this chapter, an external forcing is necessary to escape from the loop of droughts, such as the multiyear drought. Over North America, wet and warm low-level southerlies from the Gulf of Mexico, which are referred to as the Great Plain low-level jet, bring the abundant moisture from the tropical region. The wet low-level southerlies are associated with abundant precipitation, which can recover the normal climate situation.

Not only the causes of the drought and heatwaves, but the anthropogenic impacts have also been detected by the Event Attribution method. A previous study on the California drought indicated that anthropogenic warming has substantially increased the overall likelihood of extreme California droughts ([35] Willams et al. 2015).

46.8. Summary

This section addresses the flood and drought over the world under the changing climate. As shown above, the causes and temporal and spatial scales are quite regional and seasonal dependent over the world. Thus, an important, though not concrete, the summary is that it is very difficult to discuss future floods and droughts through a unified set of indicators and methods. Even if uniform indicators and methods are used, specific assessments and recommendations need to be made, taking into account regional and seasonal differences in the interpretation of the indicators and methods.

In the context of global warming, floods over some regions are associated with short-time heavy precipitation events. On the other hand, over other regions, precipitation of a future super tropical cyclone may affect floods.

Drought is sometimes associated with the long-term changes in drying trends due to an expansion of the Hadley circulation, such as the Mediterranean Sea region. On the other hand, decadal or interannual variations in the atmosphere-ocean coupling modes, which are understood as internal climate variations, can control severe drought in some regions.

It should be noted that a specific flood/drought event can be explained by the specific precipitation and the related specific atmospheric circulations. Also, a specific season of extreme flood/drought can be explained by anomalous precipitation and the related atmospheric circulations. For each event, it is difficult to separate climate change from natural variability, but a number of studies have found that the frequency of floods and droughts can vary with climate change. Thus, each specific flood/drought is partly, but certainly, affected by climate changes.

Bibliography

- [1] Trenberth KE, Smith L, Qian T et al. (2007). Estimates of the Global Water Budget and Its Annual Cycle Using Observational and Model Data. *J. Hydrometeorol.*, 8(4):758–769.
- [2] EM-DAT (2021). Disaster Year in Review 2020, Cred Crunch, 62, p. 1. <https://cred.be/sites/default/files/CredCrunch62.pdf>. Retrieved on July 8, 2021.
- [3] Burt CC (2004). "Rain and Floods", *Extreme Weather: A Guide & Record Book*, W. W. Norton & Co., pp. 123–124.
- [4] National Weather Services (2021). "Flash Flooding Definition". <https://www.weather.gov/phi/FlashFloodingDefinition>.
- [5] Papa F, Prigent C, Rossow WB (2007). Ob' River flood inundations from satellite observations: A relationship with winter snow parameters and river runoff. *J. Geophys. Res.*, 112, D18103. doi:10.1029/2007JD008451.
- [6] NOAA (2021). "Storm Surge Overview". <https://www.nhc.noaa.gov/surge/>. Retrieved on July 9, 2021.
- [7] Hungr O, Leroueil S, Picarelli L (2014). The Varnes classification of landslide types, an update. *Landslides*, 11:167–194. doi:10.1007/s10346-013-0436-y.
- [8] Gunn AM (2008). "Yellow River, China, Flood 1887 AD", *Encyclopedia of Disasters*, Greenwood Press, pp. 141–145.
- [9] Coutney C (2018). *The Nature of Disaster in China: The 1931 Yangzi River Flood*. Cambridge University Press.
- [10] Kabir MM, Saha BC, Hye JMA (2006). Cyclonic storm surge modelling for design of coastal polder. Institute of Water Modeling. <https://web.archive.org/web/20070622000638/http://www.iwmbd.org/html/PUBS/publications/P024.PDF>. Retrieved on July 9, 2021.
- [11] Muscolino MS (2014). *The Ecology of War in China*. Cambridge University Press.
- [12] Xu Y, Zhang LM, Jia J (2008). Lessons from catastrophic dam failures in August 1975 in Zhumadian, China. *GeoCongress 2008*, ASCE, pp. 162–169.
- [13] Seneviratne SI et al. (2012). Changes in climate extremes and their impacts. In: Field CB et al. (eds.) *Managing the Risks of Extreme Events*, IPCC. Cambridge University Press, pp. 109–230.

- [14] Seneviratne SI, Corti T, Davin EL et al. (2010). Investigating soil moisture–climate interactions. *Earth-Sci. Rev.*, 99(3–4):125–161.
- [15] Palmer WC (1965). Meteorological Drought. Report 45, US Weather Bureau.
- [16] Dai A (2011). Drought under global warming: A review. *WIREs Clim. Change*, 2(1):45–65.
- [17] Schneider U, Fuchs T, Meyer-Christoffer A et al. (2008). Global precipitation analysis products of the GPCC. https://opendata.dwd.de/climate_environment/GPCC/PDF/GPCC_intro_products_v2015.pdf. Retrieved on November 1, 2021.
- [18] Adler RF, Gu G, Sapiano M et al. (2017). Global precipitation during the satellite era. *Surv. Geophys.*, 38(4):679–699.
- [19] Kalnay E et al. (1996). The NCEP/NCAR 40-year reanalysis project. *Bull. Amer. Meteor.*, 77(3):437–472.
- [20] Kobayashi S et al. (2015). The JRA-55 reanalysis: General specifications. *J. Meteorol. Soc. Japan*, 93(1):5–48.
- [21] Chang DY et al. (2021). Biomass burning aerosols from Australian wildfires. *Environ. Res. Lett.*, 16(4), 044041.
- [22] Dai A (2013). Increasing drought under global warming. *Nat. Clim. Chang.*, 3:52–58. doi:10.1038/nclimate1633.
- [23] Kitoh A et al. (1997). Simulated changes in the Asian summer monsoon. *J. Meteorol. Soc. Japan*, 75(6):1019–1031.
- [24] Kamizawa N, Takahashi HG (2018). Trends in summer precipitation extremes in CMIP5. *J. Clim.*, 31(20):8421–8439. doi:10.1175/JCLI-D-17-0685.1.
- [25] Yamaji M, Takahashi HG (2014). Asymmetrical aerosol-cloud interactions. *SOLA*, 10:185–189. doi:10.2151/sola.2014-039.
- [26] Xie SP et al. (2016). Indo-western Pacific ocean capacitor. *Adv. Atmos. Sci.*, 33(4):411–432. doi:10.1007/s00376-015-5192-6.
- [27] Takahashi HG, Fujinami H (2021). Decadal enhancement of Meiyu–Baiu rainfall. *Sci. Rep.*, 11, 13665. doi:10.1038/s41598-021-93006-0.
- [28] Takaya Y et al. (2020). Enhanced Meiyu-Baiu rainfall in 2020. *Geophys. Res. Lett.*, 47(22), e2020GL090671.
- [29] Wei K et al. (2020). Catastrophic 2020 Yangtze River flooding. *The Innovation*, 1, 100038. doi:10.1016/j.xinn.2020.100038.
- [30] Sugimoto S (2020). Heavy precipitation in southwestern Japan. *SOLA*, 16:17–22. doi:10.2151/sola.2020-004.
- [31] Enomoto T, Hoskins BJ, Matsuda Y (2003). Bonin high formation mechanism. *Q. J. R. Meteorol. Soc.*, 129:157–178.

- [32] Takahashi HG et al. (2015). Role of tropical cyclones in the 2011 Thai flood. *J. Clim.*, 28(4):1465–1476. doi:10.1175/JCLI-D-14-00147.1.
- [33] Seager R, Hoerling M (2014). Origins of North American droughts. *J. Clim.*, 27(12):4581–4606. doi:10.1175/JCLI-D-13-00329.1.
- [34] Schubert SD et al. (2004). Causes of long-term drought in the U.S. Great Plains. *J. Clim.*, 17(3):485–503. doi:10.1175/1520-0442(2004)017<0485:COLDIT;2.0.CO;2.
- [35] Williams AP et al. (2015). Anthropogenic contribution to California drought. *Geophys. Res. Lett.*, 42:6819–6828. doi:10.1002/2015GL064924.